2018

Phase Transitions and Their Interaction with Dislocations in Silicon

Valery I. Levitas
Iowa State University, vlevitas@iastate.edu

Hao Chen
Iowa State University

Liming Xiong
Iowa State University, lmxiong@iastate.edu

Phase Transitions and Their Interaction with Dislocations in Silicon

Abstract
In this paper, phase transformations (PTs) in silicon were investigated through molecular dynamics (MD) using Tersoff potential. In the first step, simulations of PTs in single crystal silicon under various stress-controlled loading were carried out. Results shows that all instability points under various stress states are described by criteria, which are linear in the space of normal stresses. There is a region in the stress space in which conditions for direct and reverse PTs coincide and a unique homogeneous phase transition (without nucleation) can be realized. Finally, phase transition in bi-crystalline silicon with a dislocation pileup along the grain boundary (GB) was carried out. Results showed that the phase transition pressure first decreases linearly with the number of dislocation pileups and then reaches a plateau with the accumulation of dislocations in the pileup. The maximum reduction of phase transition pressure is 30% compared to that for perfect single crystalline silicon.

Keywords
Molecular dynamics, Phase transition criteria, Homogeneous phase transition, Triaxial loading, Phase transition pressure, Grain boundary, Dislocation pileup

Disciplines
Engineering Physics | Metallurgy | Structural Materials

Comments
This is a post-peer-review, pre-copyedit version of an article published as Levitas, Valery I., Hao Chen, and Liming Xiong. "Phase transitions and their interaction with dislocations in silicon." In *Proceedings of the International Conference on Martensitic Transformations: Chicago*, edited by A. Stebner and G. Olson. Springer, Cham, 2018: 83-87. DOI: 10.1007/978-3-319-76968-4_13. Posted with permission.

Phase Transitions and Its Interaction with Dislocations in Silicon

Valery I. Levitas[1,2], Hao Chen[3] , and Liming Xiong [3]

1) *Departments of Aerospace Engineering, Mechanical Engineering, and Material Science and Engineering, Iowa State University, Ames, IA 50011, USA.* vlevitas@iastate.edu
2) *Ames Laboratory, Division of Materials Science and Engineering, Ames, IA 50011, USA*
3) *Department of Aerospace Engineering, Iowa State University, Ames, IA 50011, USA*

Abstract

In this paper, phase transformations (PTs) in silicon was investigated through molecular dynamics (MD) using Tersoff potential. In the first step, simulations of PTs in single crystal silicon under various stress-controlled loading were carried out. Results shows that all instability points under various stress states are described by criteria, which are linear in the space of normal stresses. There is a region in the stress space in which conditions for direct and reverse PTs coincide and an –unique homogeneous phase transition (without nucleation) can be realized. Finally, phase transition in bi-crystalline silicon with a dislocation pile up along the grain boundary (GB) were carried out. Results showed that the phase transition pressure first decreases linearly with the number of dislocation pileup and then reaches a plateau with the accumulation of dislocations in the pileup. The maximum reduction of phase transition pressure is 30% comparing to that for perfect single crystalline silicon.

Keywords: molecular dynamics, phase transition criteria, homogeneous phase transition, triaxial loading, phase transition pressure, grain boundary, dislocation pileup.

1. INTRODUCTION

It is known that nonhydrostatic stresses and plastic deformation drastically reduce phase transformation pressure for various materials [1-5]. However, the reasons and mechanisms are still not completely clear. There is an analytical model [2,3,4,6,7] and phase field solutions for nucleation of a high pressure phase at the tip of strain-induced dislocation pile up, that suggests that this may be a possible mechanism for strong reduction in transformation pressure. In this paper, we will report results of some our atomistic studies. First, we will review the lattice instability criteria under six dimensional non-hydrostatic loadings [8,9]. Then we introduce silicon bi-crystal and dislocation pile up along the GB to investigate the role of dislocation activities in promoting phase transformation.

2. Simulation Method

In this work, classical MD simulations were performed using the LAMMPS package [10]. Tersoff interatomic potential is employed as the interatomic force field for the interactions between Si atoms [11]. This potential has been demonstrated to be successful in describing the transition from the diamond-cubic to beta-tin in single crystal silicon (Si I to Si II) under a uniaxial stress of _12GPa (see [12] and current results), which is close to the experimental value [13]. The majority of simulations have been performed for a Si sample containing 64,000 atoms. To prove a size-independence of the results, simulations under uniaxial loading were performed for varying sample sizes ranging from 5nm to 40nm, which contain 8,000 to 4,096,000 atoms, respectively. A time step of 1 fs was used in all simulations. The system temperature is set as T = 1K to eliminate the possibility of the occurrence of thermally activated phase transitions (PTs). Effects of the free surfaces on the PTs were excluded by employing periodic boundary conditions along all three directions. For uniaxial loading, simulations were conducted under (a) a specified first Pila-Kirchhoff stress $\boldsymbol{P}$; (b) a specified Cauchy stress $\boldsymbol{\sigma}$; and (c) a strain-controlled loading. Here the first Piola-Kirchhoff stress $\boldsymbol{P}$ was applied to the system by enforcing constant forces on the top and bottom layers of the atomistic system along the directions of compression. The Cauchy stress $\boldsymbol{\sigma}$ was applied to the system using the Berendsen algorithm [14], in which the instantaneous stress of the system was calculated using the virial formula and controlled in two steps. First, a Cauchy stress increment of 0.01 GPa was applied to the simulation cell; this was then followed by an equilibration of the entire specimen for 10 ps. In order to ensure that a desired Cauchy stress has

been achieved, the system virial stress at the end of each loading increment was calculated and was checked against the prescribed stress, assuming that the averaged Cauchy stress coincides with the virial stress [15]. It should be noted that such a weak-coupling stress-controlling strategy is different from that of using the Parinello-Rahman algorithm [16], which, in contrast, approximately controls the deviatoric component of the second Piola-Kirchhoff stress $\boldsymbol{T}$ [17]. In the strain-controlled loading, the fix deform method in LAMMPS was employed. That is, each time after the simulation box size along the main loading direction was changed at a value of 0.2 angstrom, the system was equilibrated for 100 ps. This atomistic system was equilibrated with a fixed box size along the loading direction and zero stress along the other direction. Multiaxial loading was applied to the simulation cell through controlling the normal components of the Cauchy stress utilizing the Berendsen algorithm [14]. However, shear stresses in LAMMPS cannot be applied through the Berendsen algorithm. They were applied with the Parinello-Rahman algorithm [15], which controls the deviatoric part of the second Piola-Kirchhoff stress $\boldsymbol{T}$ [16]. At the instability point, the Cauchy stress was calculated and substituted into the instability criterion.

3. Simulation Results

3.1 Instability Criteria Calibrated by Molecular Dynamics

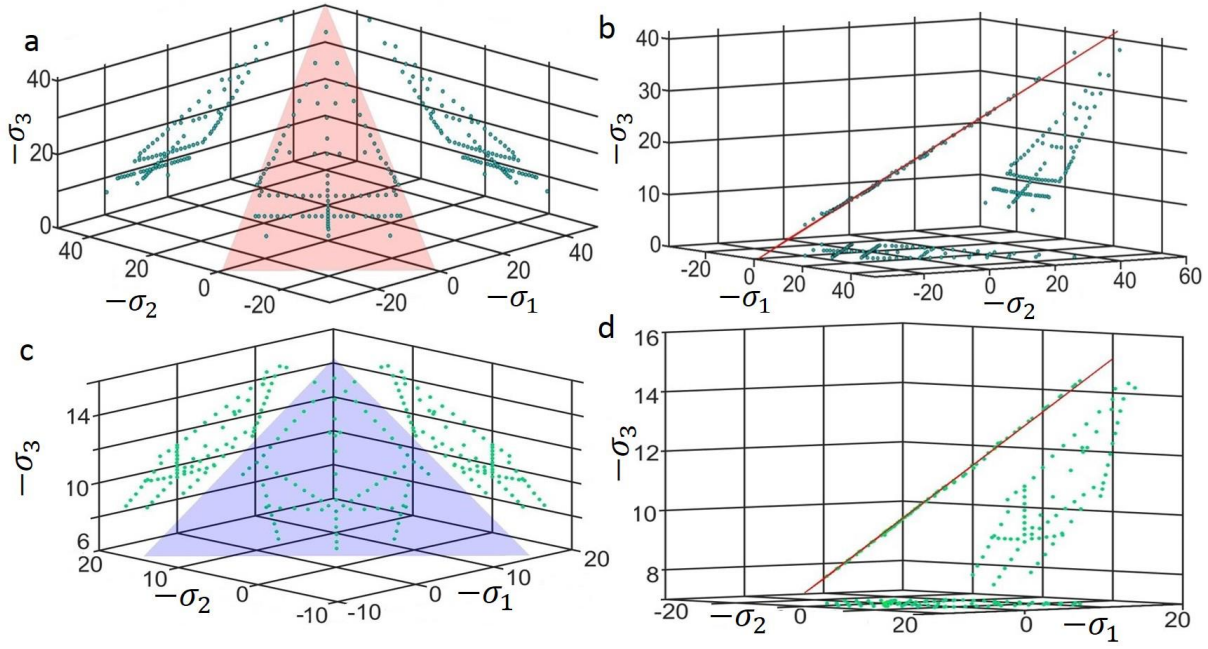

Figure 1: (A) Plane in stress space corresponding to the analytical instability criterion from [8,9] for direct Si I→Si II PT and the lattice instability points from MD simulations. (B) The plot in (A) is rotated until theoretical plane is visible as a line. (C) and (D) are the same plots as in (A) and (B) but for reverse Si II→Si I PT [9].

Using a phase field approach, the lattice instability (phase transformation) criteria for cubic-tetragonal PTs, Si I↔Si II, was derived as a linear function of three normal prescribed Cauchy stresses σ_i along cubic axes [8,9]. They are shown as the planes in Fig. 1. The negative stresses are compressive, and compressive stress σ_3 has the largest magnitude. In order to validate these lattice instability criteria, corresponding MD simulations were performed. Microstructure evolution during PTs Si I↔Si II and typical uniaxial stress - strain curves for σ, P, and the second Piola-Kirchhoff stress $\boldsymbol{T}$ for direct and reverse PTs are shown in Fig. 2 under prescribed σ, P, and displacements (strains). Under a prescribed σ, instability for the PT of Si I→Si II starts at maximum Cauchy stress (point I, Lagrangian strain E = 0.2293), i.e., at a zero elastic modulus, which is typical for a sample under a multiaxial loading as well; P and T continue growing beyond the instability point I. However, reverse PT starts at a minimum stress but nonzero value of any elastic moduli, i.e., it cannot be described by traditional zero-moduli approach. Instability is easily detected by the impossibility of equilibrating the system under fixed σ until it transforms to an

alternative phase. After instability point I, the microstructure initially evolves homogeneously, then heterogeneously with stochastic fluctuations, then with bands consisting of some intermediate phases (Fig. 2). At larger strains, bands with fully formed Si II appear and grow. However, if starting with band structure, the stress increases (i.e., strain reduces) toward instability point I, heterogeneous fluctuating structure is observed even in the vicinity of instability point I (Fig. 2). Thus, multiple solutions–including homogenous and various heterogeneous ones–are observed after instability.

The main result is that instability stresses for both direct and reverse PTs in silicon under a broad variation of all three stresses fall within a plane, see Fig. 1. Thus, it is sufficient to find just two material parameters for two different stress states in order to describe instability at any other stress states.

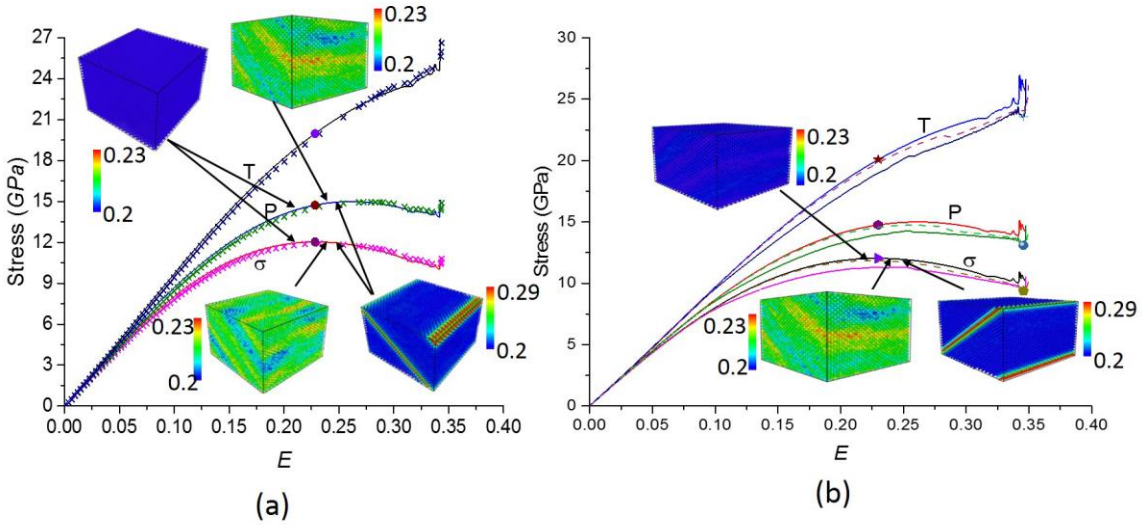

FIG. 2 Stress - Lagrangian strain E curves for uniaxial compression ($\sigma_1 = \sigma_2 = 0$) for the Cauchy σ, the first Piola-Kirchhoff P, and the second Piola-Kirchhoff stress T for direct ((a) and upper curves in (b)) and reverse (lower curves in (b)) PTs Si I↔Si II. Dots mark instability points, which correspond to stresses above (or below for reverse PT) which crystal cannot be at equilibrium at prescribed σ or multiple (homogeneous and heterogeneous) microstructures exist. After loss of stability, the microstructure initially evolves homogeneously, then heterogeneously with stochastic fluctuations, then with bands consisting of some intermediate phases and, at larger strains, bands with fully formed Si II [9].

3.2 Homogeneous hysteresis-free phase transformation and continuum of intermediate phases

For $\sigma_2 = \sigma_1$, lattice instability and initiation of PT in silicon can be described by equations $\sigma_3^d = 11.8286 + 0.6240\sigma_1$ and $\sigma_3^r = 9.3888 + 0.3840\sigma_1$, for direct and reverse PTs, respectively. Because instability lines possess different slopes in $\sigma_3 - \sigma_1$ plane (Fig. 3), they should intersect at the point $\sigma_1 = 10.1658$ and $\sigma_3 = 5.4851$. Instead, the instability line for Si I→Si II PT bends and merges with the line for Si II→Si II PT within a broad stress range. The phase equilibrium line (corresponding to the equality of the Gibbs energy of phases (Fig. 3)) is between instability lines, and consequently, it should also coincide with the merged lines. The stress hysteresis, defined as the difference in values of σ_3 between instability stresses for direct and reverse PTs for the same σ_1, decreases down to zero when σ_1 increases toward the merged region. Within the merged region, the energy barrier between phases disappears and Gibbs energy possess flat portion with constant energy between strains corresponding to each of phases. Consequently, each intermediate phase along the transformation path has the same Gibbs energy as both phases and is in an indifferent (i.e., intermediate between stable and unstable) thermodynamic equilibrium state. If one of the strains (i.e., displacement at the boundary) is prescribed, then any intermediate crystal structure can be arrested (see Fig. 4B).

Away from the merged region, when Si I becomes unstable, transformation occurs through nucleation of Si II followed by formation of multiple bands of Si II (Fig. 4A) and their growth until the completeness of PTs. This happens in a material sample under both prescribed stresses and prescribed or changing strains. Interestingly,

homogeneous intermediate structures are not observed and cannot be stabilized and studied. In contrast, within and in the close vicinity of the merged region, the transformation process is homogeneous (Fig. 4B) and each intermediate homogeneous crystal structure can be arrested and studied.

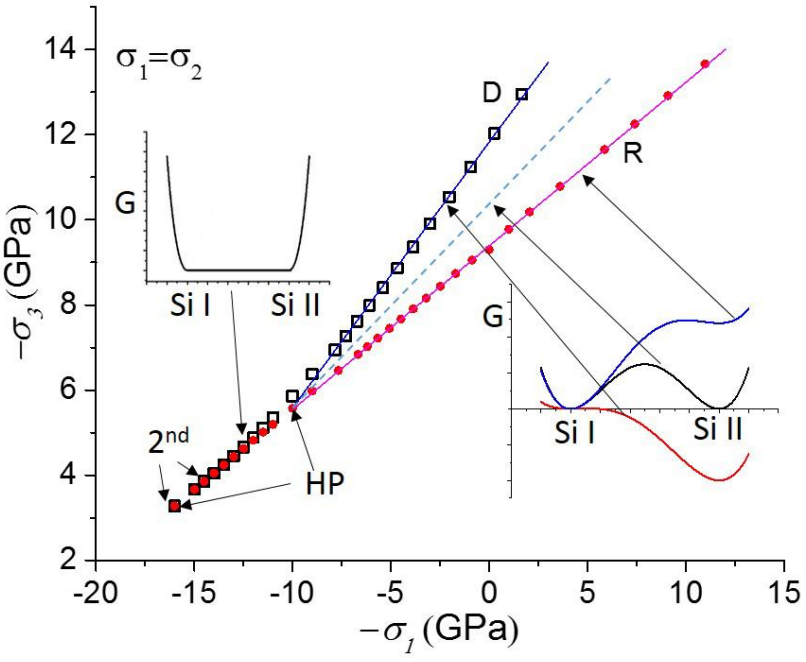

Figure 3. Relationships between stresses σ_3 and $\sigma_1 = \sigma_2$ for the crystal lattice instability for direct and reverse Si I↔Si II PTs and existence of the continuum of homogenous intermediate phases. Each instability line is related to the disappearance of the minimum in the Gibbs energy G plot for the corresponding phase. The dashed line is the tentative phase equilibrium line corresponding to equality of the Gibbs energy G of phases. For the stress states at the merge of two instability lines, Gibbs energy has a plateau with constant value leading to unique homogeneous and hysteresis-free first-order Si I↔Si II PT, with a continuum of intermediate homogeneous phases (HP), which are in indifferent thermodynamic equilibrium. With a further increase in σ_1, the first-order transformation changes to the second-order transition (designated as 2nd) and then (not shown) to a disordered phase [8].

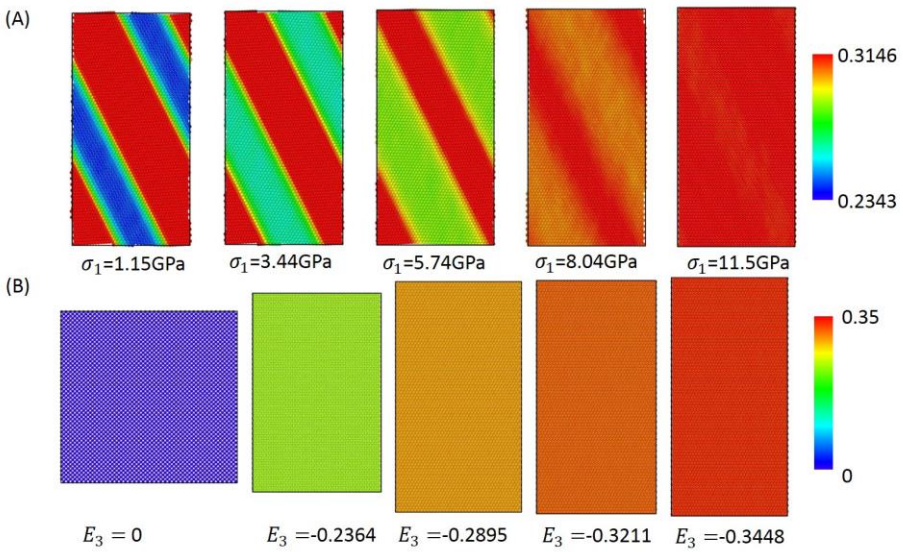

Figure 4. Nanostructure evolution in silicon during phase transformation. (A) Transformation of two-phase Si I-Si II mixture into intermediate homogeneous phase at prescribed compressive strain $E_3 = -0.31$ and increasing tensile stresses $\sigma_1 = \sigma_2$. (B) Homogeneous transformation process from Si I to Si II through continuum of homogeneous phases with increasing strain E3 at fixed stresses $\sigma_1 = \sigma_2$=11GPa. Colors characterize the local von-Mises shear strain [8].

3.3 Phase Transformation Induced by a Dislocation Pileup at the GB

Here dislocations and phase transitions simultaneously occur within one computer model. In the literature, the best potential to describe dislocation behavior in silicon is the Stillinger Weber (SW) [18] potential while the best potential to describe phase transition in silicon is the Tersoff potential [11]. We failed to find an interatomic potential in literature which can accurately describe a simultaneous occurrence of dislocations and phase transitions. One way to escape the limitation of the existing potentials is to use different potentials for different parts of the simulations [19]. In this paper, we apply the strategy similar to that in [19]. In the Grain I, where dislocations will be generated, the SW potential is used while in the Grain II, where phase transition happens, the Tersoff potential is used. We also used the Tersoff potential to commute the forces between Grain I and Grain II. In this case, dislocations are generated in the Grain I and pileup along the GB. The stress concentration in the Grain II is obvious. Thereafter, a hydrostatic pressure was applied to the sample, martensitic phase nucleate around the stress concentration and propagate along the GB. Notice that now the critical stress to nucleate the Si II phase is $45GPa$ while for perfect crystal it is $80GPa$. The nucleation pressure has been reduced, which demonstrated that the dislocation pileup plays a critical role in the nucleation of a new phase at the GB.

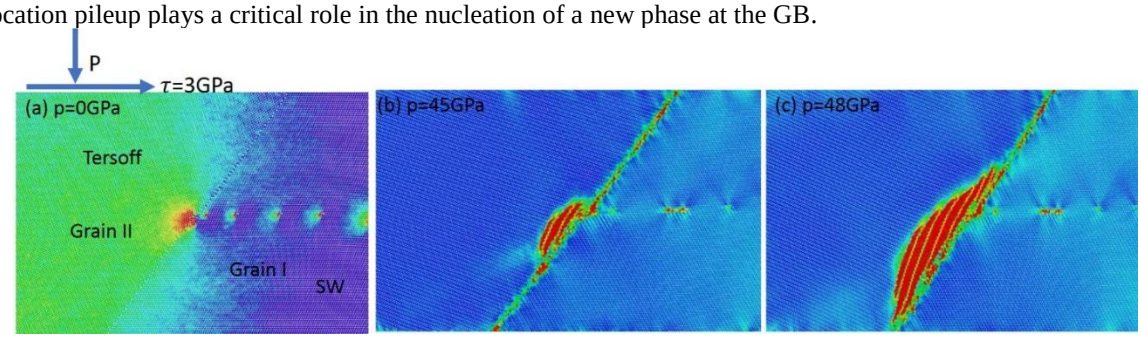

Figure 5. Nucleation of Si II at perfect 60^0 dislocation pileup. (a) along the GB. (a) Dislocations were generated in Grain I under constant shear stress $\tau = 3GPa$. (b) Hydrostatic pressure $p = 45GPa$ was applied to the sample while keeping the constant shear stress τ. The high pressure phase $Si\ II$ nucleated along the GB around the stress concentration due to dislocation pileup; (c) Martensitic phase $Si\ II$ grows along the GB.

4. Concluding remarks

In this paper, phase instability criterion is calibrated by MD simulations. Through MD simulations, homogeneous phase path through applying tension stress along the two transverse directions are found. Furthermore, dislocation pileup along the GB was generated in the simulation. It is shown that dislocation pileup can induce phase nucleation and greatly reduce the nucleation pressures.

5. Acknowledgements

The support of NSF (DMR-1434613 and CMMI-1536925), ARO (W911NF-12-1-0340), and Iowa State University (Schafer 2050 Challenge Professorship) is gratefully acknowledged.

6. References

1. Blank, VD, and Estrin, EI (2014) Phase Transitions in Solids under High Pressure. CRC Press, New York
Science and Engineering. Eds. Y. Gogotsi and V. Domnich, Inst. of Physics, Bristol, Section 3, p 159-292
2. Levitas, VI (2004) Continuum mechanical fundamentals of Mechanochemistry. In: High Pressure Surface
3. Levitas VI (2004) High-pressure mechanochemistry: conceptual multiscale theory and interpretation of experiments. Phys. Rev. B. 70:184118
4. Ji C, Levitas VI, Zhu H, Chaudhuri J, Marathe A, and Ma Y (2012) Shear-induced phase transition of nanocrystalline hexagonal boron nitride to wurtzitic structure at room temperature and low pressure. Proceedings of the National Academy of Sciences of the United States of America. 109:19108-19112
5. Levitas VI, and Shvedov LK (2002) Low pressure phase transformation from rhombohedral to cubic BN: experiment and theory. Phys. Rev. B. 65:104109
6. Levitas VI, and Javanbakht M (2014) Phase transformations in nanograin materials under high pressure and plastic shear: nanoscale mechanisms. Nanoscale 6:162-166
7. Javanbakht M, and Levitas VI (2016) Phase field simulations of plastic strain-induced phase transformations under high pressure and large shear. Phys. Rev. B. 94:214104
8. Levitas VI, Chen H, and Xiong L (2017) Triaxial-stress-induced homogeneous hysteresis-free first-order phase transformations with stable intermediate phases. Physical Review Letters. 118:025701
9. Levitas VI, Chen H, and Xiong L (2017) Lattice instability during phase transformations under multiaxial stress: modifed transformation work criterion. Physical Review B, 96:054118
10. Plimpton, S. (1995). Fast parallel algorithms for short-range molecular dynamics. Journal of computational physics, 117(1), 1-19.
11. Dodson, B. W. (1987). Development of a many-body Tersoff-type potential for silicon. Physical Review B, 35(6), 2795.
12. Mizushima, K., Yip, S., and Kaxiras, E. (1994). Ideal crystal stability and pressure-induced phase transition in silicon. Physical Review B, 50(20), 14952.
13. Golovin, Y. I. (2008). Nanoindentation and mechanical properties of solids in submicrovolumes, thin near-surface layers, and films: a review. Physics of the solid State, 50(12), 2205-2236.
14. Ryckaert, J. P., Ciccotti, G., and Berendsen, H. J. (1977). Numerical integration of the cartesian equations of motion of a system with constraints: molecular dynamics of n-alkanes. Journal of Computational Physics, 23(3), 327-341.
15. Subramaniyan, A. K., and Sun, C. T. (2008). Continuum interpretation of virial stress in molecular simulations. International Journal of Solids and Structures, 45(14), 4340-4346.
16. Martoňák, R., Laio, A., and Parrinello, M. (2003). Predicting crystal structures: the Parrinello-Rahman method revisited. Physical review letters, 90(7), 075503.
17. Miller, R. E., Tadmor, E. B., Gibson, J. S., Bernstein, N., and Pavia, F. (2016). Molecular dynamics at constant Cauchy stress. The Journal of chemical physics, 144(18), 184107.
18. Stillinger, F. H., and Weber, T. A. (1985). Computer simulation of local order in condensed phases of silicon. Physical review B, 31(8), 5262.
19. Buehler, M. J., Tang, H., van Duin, A. C., & Goddard III, W. A. (2007). Threshold crack speed controls dynamical fracture of silicon single crystals. Physical Review Letters, 99(16), 165502.